© 2020. Published by The Company of Biologists Ltd | Development (2020) 147, dev183004. doi:10.1242/dev.183004

STEM CELLS AND REGENERATION

RESEARCH REPORT

Drosophila adult muscle precursor cells contribute to motor axon pathfinding and proper innervation of embryonic muscles

Guillaume Lavergne, Monika Zmojdzian, Jean Philippe Da Ponte, Guillaume Junion and Krzysztof Jagla*

ABSTRACT

Despites several decades of studies on the neuromuscular system, the relationship between muscle stem cells and motor neurons remains elusive. Using the *Drosophila* model, we provide evidence that adult muscle precursors (AMPs), the *Drosophila* muscle stem cells, interact with the motor axons during embryogenesis. AMPs not only hold the capacity to attract the navigating intersegmental (ISN) and segmental a (SNa) nerve branches, but are also mandatory to the innervation of muscles in the lateral field. This so-far-ignored AMP role involves their filopodia-based interactions with nerve growth cones. In parallel, we report the previously undetected expression of the guidance molecule-encoding genes *sidestep* and *side IV* in AMPs. Altogether, our data support the view that *Drosophila* muscle stem cells represent spatial landmarks for navigating motor neurons and reveal that their positioning is crucial for the muscles innervation in the lateral region. Furthermore, AMPs and motor axons are interdependent, as the genetic ablation of SNa leads to a specific loss of SNa-associated lateral AMPs.

KEY WORDS: Adult muscle precursors (AMPs), Motor axon, Guidance, Side, *Drosophila*

INTRODUCTION

Axonal guidance and targeted muscle innervation represent a challenging field of particular complexity. Since the 1990s, *Drosophila* embryonic neuromuscular development has been extensively analyzed and became an attractive model for providing both a deeper understanding and the identification of numerous factors involved in axon navigation. However, most of the studies are restricted to analyzing motor neurons and their muscle targets, leaving several other potential interacting partners poorly characterized. Adult muscle precursors (AMPs), the *Drosophila* muscle stem cells, arise from the asymmetric cell divisions of a subset of muscle progenitors (Carmena et al., 1995) and are characterized by the persistent expression of the myogenic transcription factor Twist (Bate et al., 1991) and activation of the Notch pathway (Lai et al., 2000; Figeac et al., 2010). They occupy stereotypical positions in the vicinity of developing body wall muscles, stay quiescent and undifferentiated during embryonic life, and are reactivated during second larval instar (Broadie and Bate, 1991; Aradhya et al., 2015) to generate muscles of the adult fly. Strikingly, AMPs are also located in the path of intersegmental (ISN) and segmental a (SNa) motor neuron branches (Bate et al., 1991; Vactor et al., 1993). However, their role and interactions with the motor neurons have not yet been analyzed in details. Here, using an AMP sensor line that reveals cell membrane extensions, we show that the navigating ISN first contacts the dorso-lateral (DL-AMPs) and then the dorsal AMP (D-AMP) that marks the end of its trajectory. In parallel, the SNa-innervating lateral muscles target the lateral AMPs (L-AMPs). *In vivo* analyses of AMP behavior highlight an active filopodial dynamic of AMPs towards the ISN and SNa, suggesting they could guide motor axons and contribute to muscle innervations. Indeed, our data show that loss or mispositioning of L-AMPs affects SNa motor axon pathfinding and branching, leading to loss of or aberrant muscle innervation. The finding that *sidestep*- and *side IV*, which encode guidance molecules, are expressed in L-AMPs suggests their involvement in this process. Thus, proper muscle innervation does not only rely on the dialogue between the motor neurons and the muscles, but also on the AMP cells. Interestingly, the relationship between AMPs and motor nerves is not one-sided, as the SNa ensures maintenance of L-AMPs during the larval stages.

Genetics Reproduction and Development Institute (GReD), University of Clermont Auvergne, UMR - INSERM 1103, CNRS 6293, 28 place Henri-Dunant, 63000 Clermont-Ferrand, France.

*Author for correspondence (christophe.jagla@uca.fr)

K.J., 0000-0003-4965-8818

Received 23 July 2019; Accepted 21 January 2020

RESULTS AND DISCUSSION

AMPs actively interact with the motor axons

During *Drosophila* embryogenesis, we can distinguish a stereotypical pattern of AMPs per abdominal hemisegment in ventral (V-AMP), lateral (L-AMPs), dorsolateral (DL-AMPs) and dorsal (D-AMPs) positions (Fig. 1B). Here, we have investigated the relationship between AMPs and motor axons, and their dynamics, during development using embryos carrying the M6-gapGFP transgene, which allows visualization of the membrane of AMP cells (Aradhya et al., 2015). We found that the intersegmental nerve (ISN) established contacts with the DL-AMPs during the embryonic stage 13 (Fig. 1A,B) and then navigated toward the D-AMP to contact it at stage 15 (Fig. 1C,D). Within the lateral field, the segmental nerve a (SNa) is sub-divided into two branches, dorsal (D-SNa), which innervates the lateral transverse muscles (LTs 1-4), and lateral (L-SNa), which targets the segmental border muscle (SBM). The SNa sub-division takes place during stage 15 and we observed that the L-SNa branch migrated towards the L-AMPs before innervating the SBM (Fig. 1C,D). In parallel, the anterior L-AMP underwent shape changes and directional migration towards the L-SNa (Fig. 1C-C″). In a similar way, one of the DL-AMPs moves dorsally following ISN migration and the D-AMPs appear to extend toward the ISN (Fig. 1C-C″). However, AMPs survival and behavior are not affected in the absence of motor axons, as shown in the *prospero* mutant, where motor axons fail to exit the CNS (Fig. S1; Broadie and Bate, 1993). To better characterize dynamics of AMP-motor axons interactions, we used the M6-GAL4; UAS-Life-actin GFP reporter line that allows *in vivo* visualization of both the motor axons and the AMPs (Fig. 1E-L). The M6-Gal4 and M6-gapGFP lines are both driven by the same

Development (2020) 147, dev183004. doi:10.1242/dev.183004

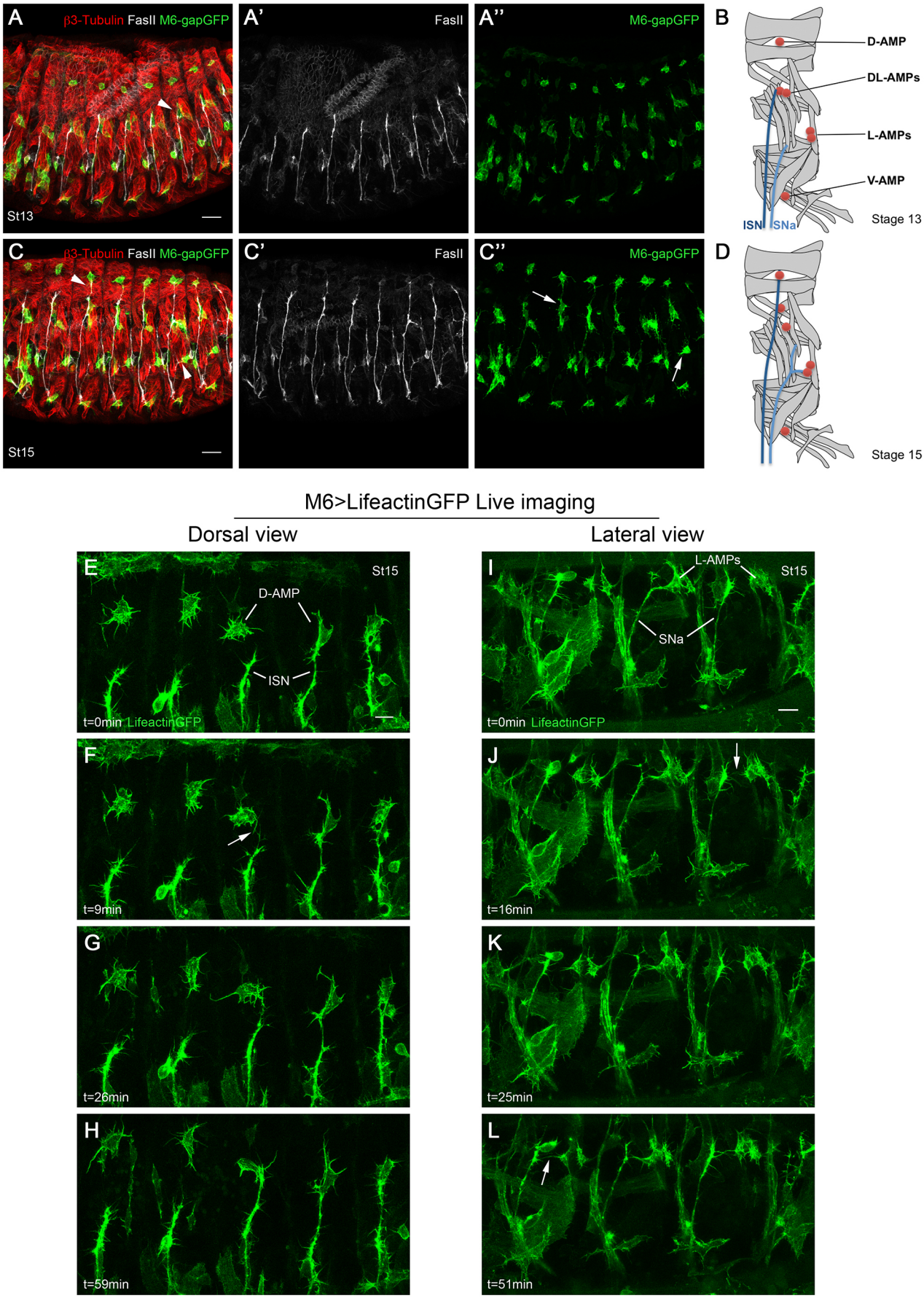

Fig. 1. See next page for legend.

Development (2020) 147, dev183004. doi:10.1242/dev.183004

Fig. 1. AMPs actively interact with the motor axons. (A-A″,C-C″) Lateral view of stage 13 (A-A″) or stage 15 (C-C″) M6-gapGFP embryos showing the embryonic pattern of motor axons (stained with anti-Fas2) and AMPs (visualized with M6-GapGFP) associated with muscles (marked by anti-β3-Tubulin). Arrowhead in A′ indicates an example of contact between DL-AMPs and the growing ISN. In C, arrowheads indicate the contact made between SNa/L-AMPs and ISN/D-AMPs. In C″, white arrows illustrate the mobility of DL-AMPs and L-AMPs in late embryogenesis. (B,D) Scheme representing muscle pattern (gray), the AMPs (red) and the two major nerve branches, ISN (dark blue) and SNa (light blue), within an abdominal hemisegment. (E-L) Selected time-points from Movies 1-3 showing *in vivo* dorsal view (E-H) or lateral view (I-L) of M6-GAL4>UAS-LifeactinGFP stage 15 embryos. The white arrows mark the first contacts between filopodia from SNa and L-AMPs (F,L). D-AMPs, L-AMPs, SNas and ISNs are indicated. Scale bars: 20 µm in A,C; 10 µm in E,I.

regulatory elements; however, the expression in motor axons, which is low and difficult to distinguish in M6-gapGFP embryos, is enhanced by the GAL4/UAS system and is clearly present in the M6>lifeActGFP context. Live imaging revealed that, among the numerous oriented cytoplasmic projections sent out by the AMPs, those contacting the growth cones of motor axons became stabilized (Fig. 1F,J,L). In particular, stabilization of filopodial connections between L-AMPs and SNa coincided with the setting of the SNa branching point and specification of its lateral branch (Fig. 1I-L). We also found oriented filopodial dynamics in the dorsal region with the contact between D-AMP projections and ISN growth cone prior to ISN migration toward the D-AMP (Fig. 1E-H). As previously demonstrated, muscle founders are needed for terminal defasciculation of the main motor axon branches (Landgraf et al., 1999). In this context, AMP positioning and the fact that they actively engage with the navigating motor axons might also participate in this process by acting as spatial check-points that either induce and or attract targeted defasciculation of ISN and SNa.

L-AMPs are required for the lateral sub-branching of the SNa

To investigate the impact of L-AMPs on the SNa pathway and branching, we first assessed the effect of a genetic ablation of the AMP cells using the M6-GAL4-driven expression of the pro-apoptotic gene *reaper*. This enabled targeted induction of apoptosis in AMPs, leading to AMP cell loss without strong defects in the ISN and SNa trajectory, despite the expression of M6-GAL4 in the motor neurons. This differential effect could be due to a lower expression level of M6-GAL4 in motor neurons than in AMPs, and/or a stronger resistance of neural cells to the Reaper-induced apoptosis. Importantly, in 86% of hemisegments (n=99), complete loss of L-AMPs was associated with absence of the lateral branch of SNa (L-SNa), strongly suggesting that L-AMPs play an instructive role in L-SNa formation and/or stabilization (Fig. 2F-J). In contrast, loss of L-SNa in hemisegments where the L-AMPs were still present occurred in 5.6% of analyzed hemisegments (n=304). The L-SNa loss in this context was thus higher than the one observed in the M6-GAL4 line with only 1.8% of hemisegments without L-SNa (n=383). To explain this difference, we cannot exclude an effect of Reaper expression in the motor system but this could also be a consequence of early stages of apoptosis in L-AMPs. Thus,

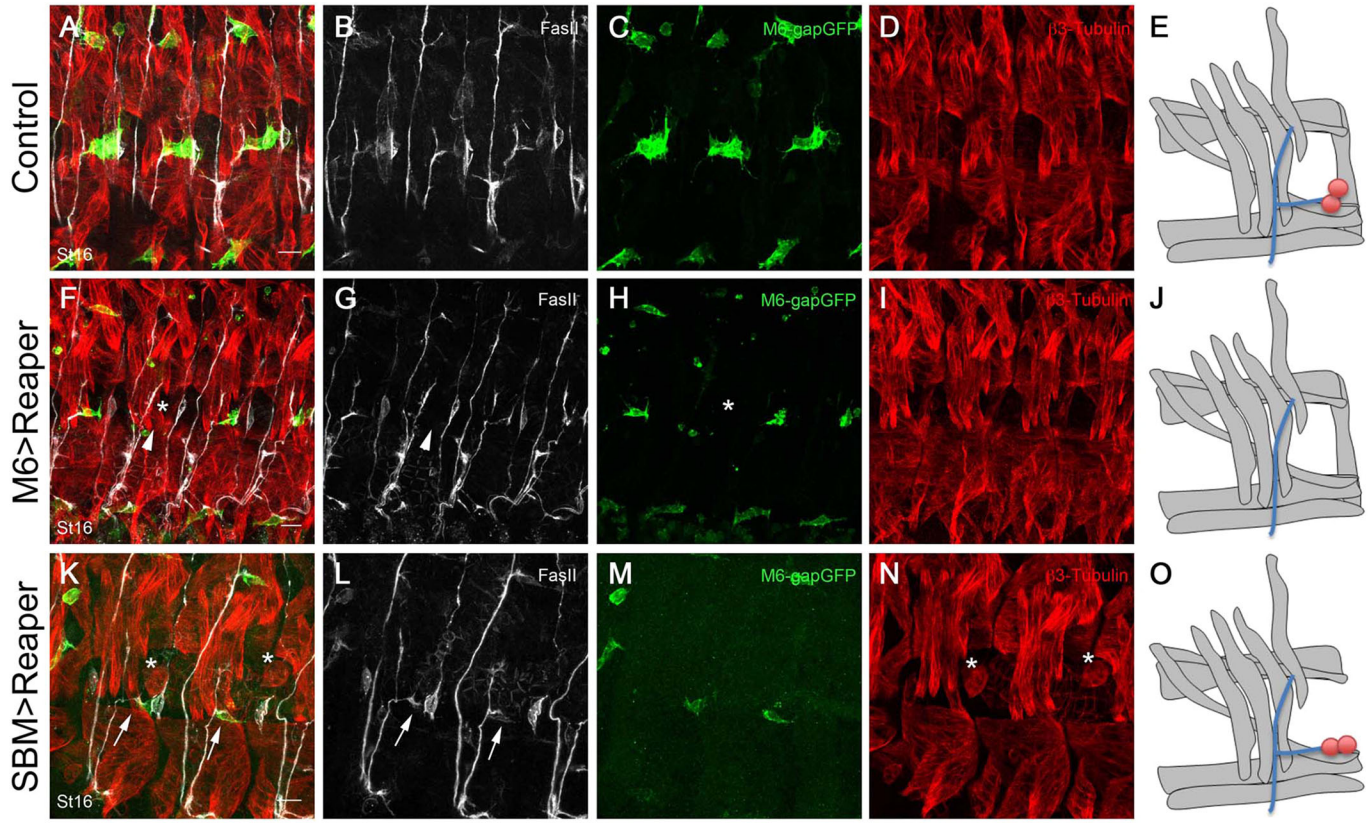

Fig. 2. Effects of targeted apoptosis on lateral SNa branching. Lateral view of a stage 16 M6-gapGFP as a control (A-D); M6-gapGFP;M6-GAL4>UAS-Reaper (F-I) and M6-gapGFP;SBM-GAL4>UAS-Reaper (K-N) embryos. (F-I) Complete apoptosis of L-AMPs is observed in one hemisegment marked by a white asterisk. The same hemi-segment also displays a loss of L-SNa (white arrowhead). (K-N) Apoptosis of SBM muscle is marked by white asterisks. Persistence of the L-SNa can be observed (white arrows) in contact with remnant L-AMP even when the SBM is missing. The length of the SNa appears dependent of the positioning of the L-AMPs. (E,J,O) Results are illustrated by recapitulative schemes with muscles in gray, AMPs in red and SNa in blue. Scale bars: 10 µm.

Development (2020) 147, dev183004. doi:10.1242/dev.183004

M6-GAL4-induced apoptosis created a context in which loss of the L-SNa branch was observed in L-AMP-devoid segments where the L-SNa target muscle (SBM) was still present (Fig. 2F-J). This suggests that L-SNa branch formation might not be dependent on its muscle target, and so prompted us to test whether the L-SNa would form or persist in an SBM-devoid context. We targeted *reaper* expression to the developing SBM using the SBM(lbl)-GAL4 driver (gift from A. Michelson, Howard Hughes Medical Institute, Boston, USA; Busser et al., 2012). The SBM(lbl)-GAL4-driven apoptosis resulted in a systematic loss of the SBM and only sporadic loss of the L-AMPs [12% hemisegments (*n*=107)]. In the SBM-devoid context but with L-AMP cells correctly located, the L-SNa branch was still present [73% of hemisegments (*n*=107, Fig. 2K-O)]. Additionally, in a subset of SBM-deficient embryos, L-AMPs shifted toward the navigating SNa, leading to a shortened L-SNa [13% of the hemisegments (*n*=107, Fig. 2L)]. These observations thus suggest an instructive role for AMPs in L-SNa establishment, and reveal that SBM might not be needed for this process and is at least dispensable for its stabilization. To further test the role of L-AMPs in lateral defasciculation of the SNa, we analyzed different genetic contexts in which AMP specification is affected. We first induced a perturbation of asymmetric cell divisions. To adversely affect divisions of progenitor cells that give rise to AMPs, we ectopically expressed the asymmetry determinant Numb using the pan-mesodermal driver Twist-GAL4 (Ruiz Gómez and Bate, 1997). In the lateral region, this led predominantly to the loss of one of the L-AMPs and a duplication of the SBM with no major impact on L-SNa formation [1.9% (*n*=518) of hemisegments without the L-SNa] compared with the control Twist-GAL4 line [1.4% (*n*=506)]. However, in a small subset of hemisegments [1.3% (*n*=518)], we observed loss of both L-AMPs but not SBM (often duplicated) (Fig. 3B-B″). In this rare context (*n*=17), the L-SNa was absent in 88% of hemisegments (Fig. 3B-B″), supporting the view that L-AMPs are required for L-SNa branching. These findings are also consistent with the effects of generalized mesodermal expression of the identity gene *Pox meso* (*Poxm*), which can lead to a loss of L-AMPs (Duan et al., 2007) without affecting SBM [30% of hemisegments (*n*=324)]. In such a context, the L-SNa formation is impaired in 89% of L-AMP-devoid segments (*n*=97, Fig. 3C-C″) against 37% in random Twi>Poxm hemisegments (*n*=324).

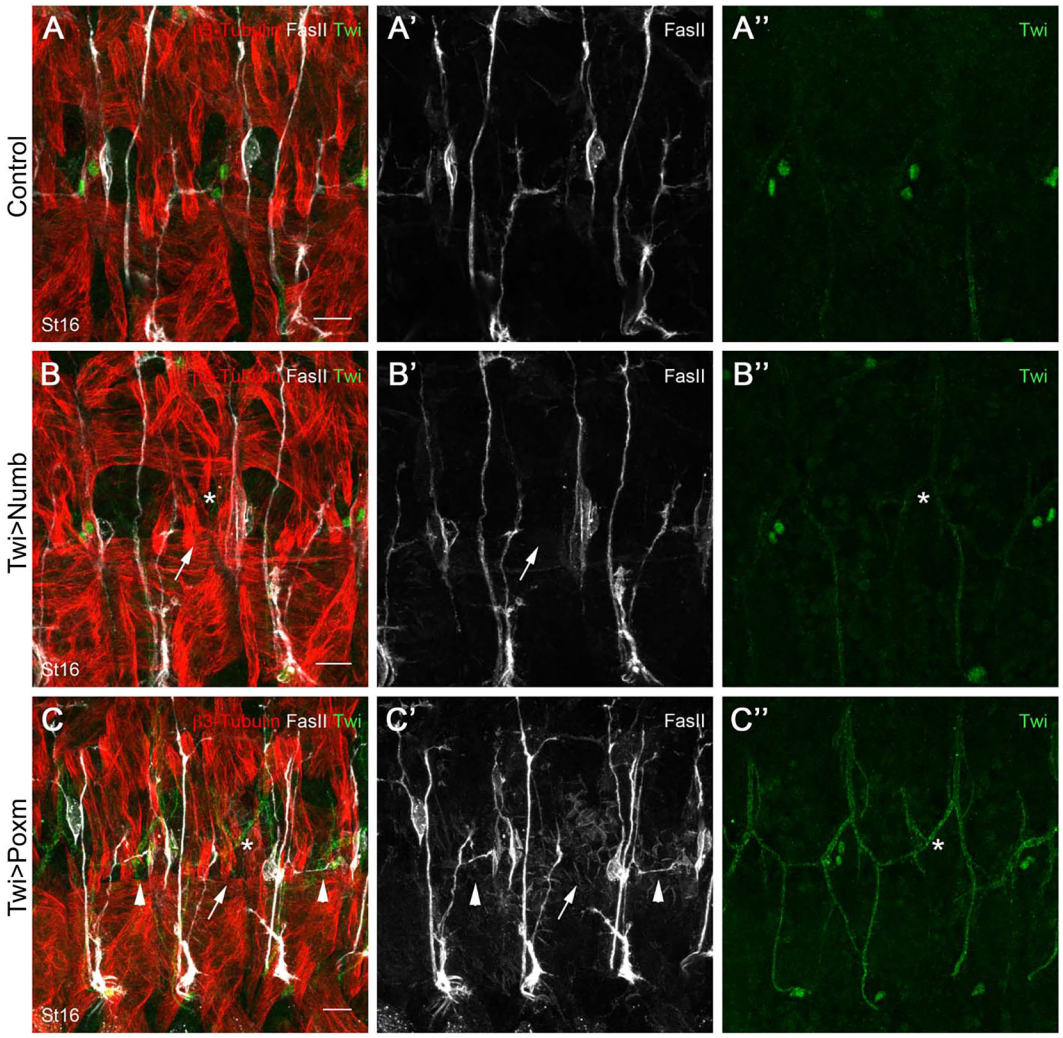

Fig. 3. Specification of L-AMPs is required for the formation of the L-SNa. Lateral view of either Twist-GAL4 (A-A″), Twist-GAL4>UAS-Numb (B-B″) or Twist-GAL4>UAS-Pox meso (C-C″) stage 16 embryos. AMPs are revealed by staining using the Twist antibody shown in green. Ectopic expression of Numb and Pox meso in the mesoderm is sufficient to affect the specification of AMPs. Absence of L-AMPs in a given hemisegment is marked with a white asterisk (B″,C″). Segments lacking L-AMPs also present absence of L-SNa indicated with a white arrow (B′,C′). (C) White arrowheads indicate dorsally mispositioned L-AMPs and the resulting L-SNa stabilized at a more dorsal position than in control segments. Scale bars: 10 µm.

Development (2020) 147, dev183004. doi:10.1242/dev.183004

Interestingly, pan-mesodermal expression of *Pox meso* can also induce misplacement of L-AMPs along the SBM, leading to aberrant L-SNa trajectory (Fig. 3C-C″). Hence, L-AMPs and their spatial positioning appear crucial to achieve the formation and correct pathfinding of the L-SNa.

AMPs express *sidestep*, which is involved in motor axon guidance

The findings described above suggest that L-AMPs are a source of attractive signals that promote lateral sub-branching of the SNa, making it competent to innervate the SBM. Interestingly, the SBM is the only lateral muscle innervated by the Connectin-positive SNa, which does not express this homophilic target recognition molecule (Nose et al., 1992, 1997). In such a context, L-AMP-mediated lateral sub-branching of SNa offers a way to drive L-SNa to its specific muscle target. As L-AMPs seem not to express Connectin either (Fig. S2), in contrast to previous suggestions (Meadows et al., 1994), their role in attracting SNa and inducing the L-SNa sub-branching might rely on other guidance molecules.

It has been previously shown that the mutants of *sidestep* and *beat-1a*, which encode interacting membrane proteins of the immunoglobulin superfamily, displayed loss of L-SNa, a phenotype similar to the one observed when L-AMPs are missing (Fambrough and Goodman, 1996; Sink et al., 2001). However, the mechanisms leading to the loss of the L-SNa in *sidestep* and *beat-1a* mutants have not been elucidated. In addition, the embryonic expression pattern of *sidestep* has been only partially characterized (Sink et al., 2001; Siebert et al., 2009). By using *in situ* hybridization, we found that *sidestep* mRNA is strongly enriched in all the AMPs, suggesting its potential involvement in the dialogue between AMPs and motor axons (Fig. S3). We therefore decided to test Sidestep protein distribution at the time when L-SNa sub-branching is taking place. By examining stage 14 to 15 embryos, we found a previously unreported faint and transient expression of Sidestep specifically in L-AMPs (Fig. S4A,A′). To confirm this observation, we analyzed the expression of Sidestep in a mutant for *beat-1a*. It has been reported (Siebert et al., 2009) that the contact of Beat-1a-expressing motor axons with Sidestep-expressing cells leads to a negative regulation of the expression of *sidestep*. If this contact is missing, cells normally expressing *sidestep* transiently and at a low level will continue to do so, leading to continuous and higher Sidestep level in these cells. Analyses of *beat-1a* mutants confirmed that the L-AMPs are Sidestep-expressing cells and that Sidestep expression onset coincides with L-SNa sub-branching (Fig. S4B-C′). The high Sidestep expression resulting from the lack of *beat-1a* was still detected in late-stage embryos in which it became gradually restricted to the most anterior L-AMPs (Fig. S4D,D′). This late differential Sidestep expression may point to a leading role for the anterior L-AMPs in the process of interaction with SNa and in its lateral sub-branching. Additionally, an increased Sidestep expression in L-AMPs was also observed in SNa-devoid *pros* mutants and in the Duf-GAL4; UAS-NetrinB (NetB) context (Fig. S5). Importantly, the SBM does not express Sidestep, making the L-AMPs the only Sidestep-expressing cells in the L-SNa pathway. Thus, this newly reported expression pattern suggests that L-AMPs could attract the L-SNa through the temporally and spatially restricted expression of *sidestep*.

Interestingly, the *sidestep* mutants also display a stall phenotype of the ISN (Sink et al., 2001) suggestive of a potential role of the D-AMPs. Indeed, we observe that the aberrantly located D-AMPs, after the mesodermal overexpression of the activated form of the Notch receptor (NICD), are able to attract the ISN, suggesting that they are a source of guiding signals (Fig. S6). However, because we detect only faint *sidestep* transcript expression in D-AMPs (Fig. S3) and are unable to detect Sidestep protein, we expect that other guiding cues may be in play. It is important to notice that to visualize the attractive potential of mis-positioned D-AMPs we induced pan-mesodermal expression of NICD via a GAL4/UAS system known to be thermo-sensitive. As described previously (Landgraf et al., 1999), high mesodermal expression of NICD induced at 29°C leads to the loss of majority of muscles but, as we show here, several muscles persist in Twi-GAL4;UAS-NICD embryos incubated at 25°C, thus allowing us to uncouple effects of delocalized D-AMPs from potential influence of muscles loss on ISN trajectories (Fig. S6). However, loss of D-AMPs, here observed in a *Poxm* gain-of-function context, appears to have only a minor effect on the capacity of ISN motor axons to target dorsal muscles, which are correctly innervated by the ISN in 65% of hemisegments without D-AMP (n=110, Fig. S6). These results highlight differential requirements of AMPs for motor axons defasciculation and navigation with L-AMPs being mandatory for L-SNa branching and D-AMPs acting as guiding cells for the ISN. However, the functional significance underlying the guidance of motor nerves by muscle stem cells remains to be determined.

It is also important to state that the loss of L-SNa in the *sidestep* mutants is not fully penetrant (observed in less than 10% of hemisegments, Sink et al., 2001), suggesting that *sidestep* is not the only player in L-SNa sub-branching. This could be due to functional redundancy between several members of Side and Beat families comprising 8 and 14 members, respectively (Özkan et al., 2013). Expression and function of Side and Beat family members remain largely unexplored, but the fact that Sidestep labels L-AMPs and its paralog, *side VI*, is expressed in the DL-AMPs (Li et al., 2017) suggests there might be a ‘Side expression code’ that operates in AMPs and makes them competent to interact with navigating motor axons. In support of this hypothesis, we found that *side IV*, another member of the Side family, is also expressed in AMPs with a higher transcript levels detected in L-AMPs (Fig. S7), suggesting it could contribute to the interactions between L-AMPs and the SNa. To gain insight into AMP functions of *sidestep* and *side IV* in setting interactions with motor neurons, the selective AMP-targeting tools need to be developed to generate AMP-specific mutant rescue.

The SNa is required for maintenance of associated L-AMPs at the larval stage

It has previously been shown that the nervous system is required for the establishment of the adult muscle pattern (Currie and Bate, 1995) and that motor axons serve as a support for migration of AMPs during larval and pupal development (Currie and Bate, 1991). More recently, it has also been suggested that the nervous system could be involved in the selection of founder cells from the pool of AMPs (Sarkissian et al., 2016). Here, we took advantage of a previously described genetic context (pan-muscular expression of NetB) to affect the SNa (Winberg et al., 1998) and test impact of SNa loss on L-AMPs. In stage 16 DUF>NetB embryos, loss of the SNa observed in 84% of the hemisegments (n=125) does not affect the number of L-AMPs. However, in surviving 3rd instar larvae in hemisegments lacking the SNa, number of L-AMPs is dramatically reduced (Fig. 4). Interestingly, we observed a specific depletion of normally associated with SNa anterior L-AMPs (complete loss in 10 out of 26 hemisegments analyzed), while the posterior L-AMPs associated with the transverse nerve (TN) remained unaffected (Fig. 4). Thus, our data provide evidence for a cross-talk between AMPs and motor axons, with the AMPs attracting navigating motor

Development (2020) 147, dev183004. doi:10.1242/dev.183004

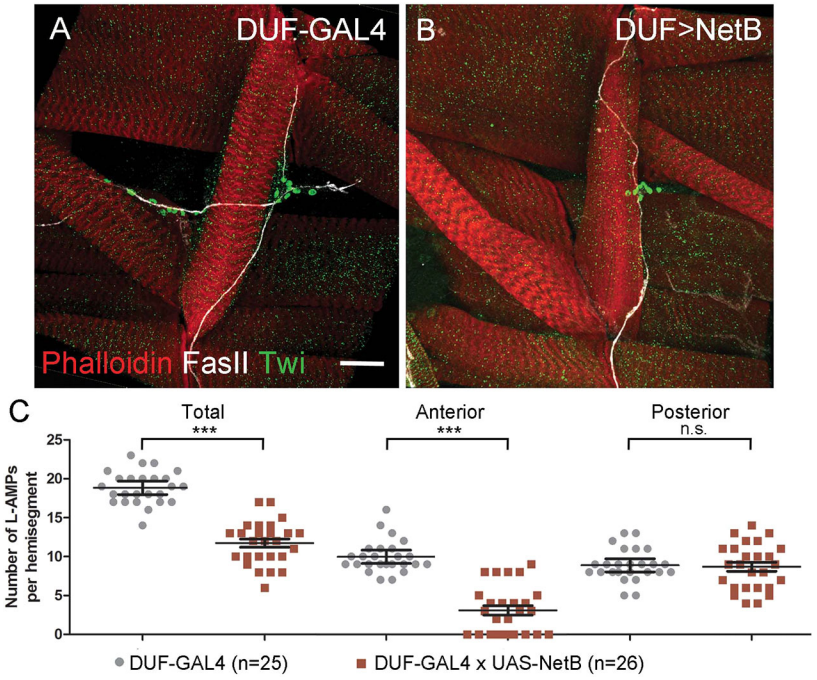

Fig. 4. Absence of SNa causes specific loss of anterior L-AMPs during larval stages. (A,B) Flat preparations of DUF-GAL4 and DUF>NetB mid-stage-matched third instar larvae stained for Twist (green) labeling AMP nuclei, Fas2 revealing the nerve braches and phalloidin (magenta) labeling the larval muscles. Both anterior and posterior L-AMPs groups are present in the control line and associated with the L-SNa and the TN, respectively (A). Overexpression of NetB in the muscles (B) leads to the loss of L-SNa correlated with the absence of the anterior group of L-AMPs. (C) Graphical representation of the mean number of L-AMPs for each experiment±s.e.m. Individual data points are indicated. Overexpression of NetB is associated with a specific reduction of anterior L-AMPs number spanning from depletion to complete loss of L-AMPs, ***$P \leq 0.001$. Interestingly, the groups of L-AMPs showing no reduction in the DUF>NetB condition were associated with a persisting L-SNa. Scale bar: 30 µm.

axons, which in turn are required for AMP maintenance during larval stages. The loss of anterior L-AMPs in SNa-devoid larva suggests that SNa-derived signals promote survival of associated L-AMPs, but precise underlying mechanisms remain to be elucidated.

Thus, in *Drosophila*, the dynamic interactions and close association between AMPs and the motor axon network contribute to setting ISN trajectory and are required for SNa sub-branching and proper innervation of lateral muscles, which is itself needed in larvae for the maintenance of anterior L-AMPs. In vertebrates, it has previously been described that muscle pioneers can impact motor axon pathfinding in zebrafish (Melançon et al., 1997) and more recently in mice that muscle stem cells activate and contribute to neuromuscular junction regeneration in response to denervation (Liu et al., 2015), and that depletion of muscle stem cells induced neuromuscular junction degeneration (Liu et al., 2017). This study, conducted in *Drosophila*, represents the first demonstration that, during development of neuromuscular system, muscle stem cells interact with motor neurons and contribute to proper muscle innervation.

MATERIALS AND METHODS

Counting and statistical analyses

Embryonic hemisegments A2 to A6 were counted in random stage 16 embryos from a given genotype. For larvae analysis, at least eight larvae were dissected per genotype and the lateral AMP groups were used for counting (sample sizes for each genotype are indicated in Fig. 4). All statistical analyses were performed using GraphPad Prism v5.02 software. Statistical significance (Mann–Whitney *U*-test) is denoted by ***$P<0.001$.

Drosophila lines

Drosophila stocks were maintained at 25°C. The M6-gapGFP (Aradhya et al., 2015) strain was used as control. Mutant strains used were *prosp*^{17} (BL5458), *beat*^{C163} (BL4742) and *beat*^{3} (BL4748). The targeted expression experiments were performed using the UAS-GAL4 system (Brand and Perrimon, 1993) on the following GAL4 and UAS lines: M6-GAL4 (generated in the lab) and SBM-GAL4 (kindly provided by A. Michelson, Howard Hughes Medical Institute, Boston, USA); DUF-GAL4 (kindly provided by M. Ruiz Gómez, Consejo Superior de Investigaciones Científicas, Madrid, Spain); Twist-GAL4 (kindly provided by M. Frasch, Friedrich-Alexander-University of Erlangen-Nürnberg, Germany); UAS-Poxm (kindly provided by M. Noll, University of Zurich, Switzerland); UAS-NetB (kindly provided by T. Kidd, University of Nevada, Reno, USA); UAS-Numb (FlyORF:F003181), UAS-Reaper (BL5824), UAS-LifeActGFP (BL58718) from Bloomington Stock Center. Mutant strains were balanced with CyO ActinGFP and TM6B KrGFP, homozygous mutant embryos were selected by absence of corresponding GFP staining. All GAL4-UAS crosses were performed at 25°C.

Immunohistochemical staining and live imaging

Staged embryos were dechorionated, fixed, blocked for 1 h at room temperature in 20% horse serum in PBT and then incubated with primary (Table S1) and secondary antibodies according to a standard procedure (Lavergne et al., 2017). Larvae dissection and immunostaining were performed as previously described (Lavergne et al., 2017). The primary antibodies used were: goat anti-GFP (1:500, Abcam, ab 5450), phalloidin-TRITC (1:1000, Sigma, P1951), guinea-pig anti-Twi (1:1000, kindly provided by R. Zinzen, Max Delbrück Center for Molecular Medicine, Berlin, Germany), rabbit anti-β3Tubulin (1:2000, kindly provided by R. Renkawitz-Pohl, University of Marburg, Germany); and mouse anti-Fas2 (1D4; 1:400), mouse anti-Con (C1.427; 1:50) and mouse anti-Side (9B8; 1:50) from the Developmental Studies Hybridoma Bank (University of Iowa, USA). Secondary antibodies were: donkey anti-rabbit, donkey anti-guinea pig, donkey anti-goat and donkey anti-mouse (Jackson Immuno Research Laboratories) conjugated to Alexa 488, Cy3 or Cy5 fluorochromes (1:300). Labeled embryos were analyzed using a Leica SP8 confocal microscope equipped with a HyD detector, with a 40× objective. Images were processed using ImageJ. *In vivo* imaging of M6>LifeActGFP embryos was performed from stage 14 to 16 over 2 h. Films were acquired on a Leica SP8 confocal microscope and analyzed using Imaris software (Bitplane).

DIG-RNA probe synthesis

Probes were synthesized by PCR on cDNA using the following primers: *side IV* forward, CAATTCCCGGCTAATGTGCG; *side IV* reverse, GCGCAATGTGACCGGATTAC; *sidestep* forward, CCAAGACAAACCGGCAACAG; *sidestep* reverse, GTCCACCCCTCACTTGACAG. Digoxigenin-labeled RNA probes were prepared using RNA labeling mixture (Roche) and T7 RNA polymerase (Roche) according to the manufacturer's instructions. After RNA synthesis, template DNA was degraded using 2 µl of RNase-free DNase I (Roche). Probes were not carbonated. RNA was precipitated at −20°C overnight by adding 1/10 volumes of 3 M NaAc (pH 5.2), 1/5 volumes of 6 M LiCl, 200 µg tRNA as carrier and 5 volumes of

absolute ethanol. After washing in 70% ethanol, pellets were resuspended in 100 µl of Hyb-A buffer (50% formamide, 5× SSC, 100 µg/ml salmon sperm, 0.1% Tween-20 and 50 µg/ml heparin) by incubation for 10 min at 37°C and pipetting.

In situ hybridization

Fixed dechorionated embryos (incubated for 20 min with 4% formaldehyde, stored in methanol or ethanol at −20°C) were transferred to a 1.5 microfuge tube, washed in 1 ml PBT (PBS with 0.1% Tween-20) with decreasing proportions of methanol (70%, 50% and 30%) for 5 min each time at room temperature, and then washed twice in PBT alone. We then performed a post-fixation step for 20 min in 4% formaldehyde in PBT. Immediately after this, embryos are washed five times with PBT for 5 min, then once in 1:1 PBT/Hyb-B (50% formamide and 5× SSC) and once in Hyb-B. The embryos were pre-hybridized in Hyb-A (50% formamide, 5× SSC, 100 µg/ml salmon sperm, 0.1% Tween 20 and 50 µg/ml heparin) at 56°C for at least 3.5 h, before adding the denatured (10 min at 80°C followed by incubation on ice) DIG-RNA probe diluted 1:50 in Hyb-A solution. We then added the diluted probe in 250 µl of total volume to the embryos. After incubation overnight at 56°C, embryos were washed six times with Hyb-B at the same temperature, the first three times for 30 min and the second three times for 1 h. Then we performed 15-min washes at room temperature with increasing proportions of PBT (20%, 50% and 80%) and finally four washes with PBT alone. The probe was detected using peroxidase-conjugated antibodies (Roche) after pre-blocking twice for 30 min in western-blot blocking reagent (Roche) diluted 1:5 in PBT. Incubation with antibodies anti-DIG POD and anti-GFP (goat) was performed overnight at 4°C and then embryos were washed six times with PBT for 20 min at room temperature before proceeding with the TSA-plus Tyramide fluorescence system (Perkin Elmer). Secondary antibody (anti-goat Alexa-488) was then added for 2 h at room temperature and after three washes for 20 min with PBT, embryos were mounted on slides.

Competing interests

The authors declare no competing or financial interests.

Author contributions

Conceptualization: G.L., K.J.; Methodology: G.L., M.Z., J.P.D.P., G.J.; Formal analysis: M.Z.; Investigation: G.L., M.Z., G.J.; Resources: G.L., K.J.; Writing - original draft: G.L.; Writing - review & editing: K.J.; Supervision: K.J.; Funding acquisition: K.J.

Funding

This work was supported by the Association Française contre les Myopathies-Téléthon (MyoNeurAlp Strategic Program), the Agence Nationale de la Recherche (Tefor Infrastructure Grant), the iSITE project CAP2025, and the Fondation pour la Recherche Médicale (Equipe FRM Award).

Supplementary information

Supplementary information available online at
http://dev.biologists.org/lookup/doi/10.1242/dev.183004.supplemental

References

Aradhya, R., Zmojdzian, M., Da Ponte, J. P. and Jagla, K. (2015). Muscle niche-driven insulin-Notch-Myc cascade reactivates dormant adult muscle precursors in Drosophila. *eLife* **4**, e08497. doi:10.7554/eLife.08497

Bate, M., Rushton, E. and Currie, D. A. (1991). Cells with persistent twist expression are the embryonic precursors of adult muscles in Drosophila. *Development* **113**, 79-89.

Brand, A. H. and Perrimon, N. (1993). Targeted gene expression as a means of altering cell fates and generating dominant phenotypes. *Development* **118**, 401-415.

Broadie, K. S. and Bate, M. (1991). The development of adult muscles in Drosophila: ablation of identified muscle precursor cells. *Development* **113**, 103-118.

Broadie, K. and Bate, M. (1993). Muscle development is independent of innervation during Drosophila embryogenesis. *Development* **119**, 533-543.

Busser, B. W., Taher, L., Kim, Y., Tansey, T., Bloom, M. J., Ovcharenko, I. and Michelson, A. M. (2012). A machine learning approach for identifying novel cell type-specific transcriptional regulators of myogenesis. *PLoS Genet.* **8**, e1002531. doi:10.1371/journal.pgen.1002531

Carmena, A., Bate, M. and Jiménez, F. (1995). Lethal of scute, a proneural gene, participates in the specification of muscle progenitors during Drosophila embryogenesis. *Genes Dev.* **9**, 2373-2383. doi:10.1101/gad.9.19.2373

Currie, D. A. and Bate, M. (1991). The development of adult abdominal muscles in Drosophila: myoblasts express twist and are associated with nerves. *Development* **113**, 91-102.

Currie, D. A. and Bate, M. (1995). Innervation is essential for the development and differentiation of a sex-specific adult muscle in Drosophila melanogaster. *Development* **121**, 2549-2557.

Duan, H., Zhang, C., Chen, J., Sink, H., Frei, E. and Noll, M. (2007). A key role of Pox meso in somatic myogenesis of Drosophila. *Development* **134**, 3985-3997. doi:10.1242/dev.008821

Fambrough, D. and Goodman, C. S. (1996). The Drosophila beaten path gene encodes a novel secreted protein that regulates defasciculation at motor axon choice points. *Cell* **87**, 1049-1058. doi:10.1016/S0092-8674(00)81799-7

Figeac, N., Jagla, T., Aradhya, R., Da Ponte, J. P. and Jagla, K. (2010). Drosophila adult muscle precursors form a network of interconnected cells and are specified by the rhomboid-triggered EGF pathway. *Development* **137**, 1965-1973. doi:10.1242/dev.049080

Lai, E. C., Bodner, R. and Posakony, J. W. (2000). The enhancer of split complex of Drosophila includes four Notch-regulated members of the bearded gene family. *Development* **127**, 3441-3455.

Landgraf, M., Baylies, M. and Bate, M. (1999). Muscle founder cells regulate defasciculation and targeting of motor axons in the Drosophila embryo. *Curr. Biol.* **9**, 589-592. doi:10.1016/S0960-9822(99)80262-0

Lavergne, G., Soler, C., Zmojdzian, M. and Jagla, K. (2017). Characterization of Drosophila muscle stem cell-like adult muscle precursors. *Methods Mol. Biol.* **1556**, 103-116. doi:10.1007/978-1-4939-6771-1_5

Li, H., Watson, A., Olechwier, A., Anaya, M., Sorooshyari, S. K., Harnett, D. P., Lee, H.-K. P., Vielmetter, J., Fares, M. A., Garcia, K. C. et al. (2017). Deconstruction of the beaten path-Sidestep interaction network provides insights into neuromuscular system development. *eLife* **6**, e28111. doi:10.7554/eLife.28111

Liu, W., Wei-LaPierre, L., Klose, A., Dirksen, R. T. and Chakkalakal, J. V. (2015). Inducible depletion of adult skeletal muscle stem cells impairs the regeneration of neuromuscular junctions. *eLife* **4**, e09221. doi:10.7554/eLife.09221

Liu, W., Klose, A., Forman, S., Paris, N. D., Wei-LaPierre, L., Cortés-Lopéz, M., Tan, A., Flaherty, M., Miura, P., Dirksen, R. T. et al. (2017). Loss of adult skeletal muscle stem cells drives age-related neuromuscular junction degeneration. *eLife* **6**, e26464. doi:10.7554/eLife.26464

Meadows, L. A., Gell, D., Broadie, K., Gould, A. P. and White, R. A. (1994). The cell adhesion molecule, connectin, and the development of the Drosophila neuromuscular system. *J. Cell Sci.* **107**, 321-328.

Melançon, E., Liu, D. W. C., Westerfield, M. and Eisen, J. S. (1997). Pathfinding by identified zebrafish motoneurons in the absence of muscle pioneers. *J. Neurosci.* **17**, 7796-7804. doi:10.1523/JNEUROSCI.17-20-07796.1997

Nose, A., Mahajan, V. B. and Goodman, C. S. (1992). Connectin: a homophilic cell adhesion molecule expressed on a subset of muscles and the motoneurons that innervate them in Drosophila. *Cell* **70**, 553-567. doi:10.1016/0092-8674(92)90426-D

Nose, A., Umeda, T. and Takeichi, M. (1997). Neuromuscular target recognition by a homophilic interaction of connectin cell adhesion molecules in Drosophila. *Development* **124**, 1433-1441.

Özkan, E., Carrillo, R. A., Eastman, C. L., Weiszmann, R., Waghray, D., Johnson, K. G., Zinn, K., Celniker, S. E. and Garcia, K. C. (2013). An extracellular interactome of immunoglobulin and LRR proteins reveals receptor-ligand networks. *Cell* **154**, 228-239. doi:10.1016/j.cell.2013.06.006

Ruiz Gómez, M. and Bate, M. (1997). Segregation of myogenic lineages in Drosophila requires numb. *Development* **124**, 4857-4866.

Sarkissian, T., Arya, R., Gyonjyan, S., Taylor, B. and White, K. (2016). Cell death regulates muscle fiber number. *Dev. Biol.* **415**, 87-97. doi:10.1016/j.ydbio.2016.04.018

Siebert, M., Banovic, D., Goellner, B. and Aberle, H. (2009). Drosophila motor axons recognize and follow a Sidestep-labeled substrate pathway to reach their target fields. *Genes Dev.* **23**, 1052-1062. doi:10.1101/gad.520509

Sink, H., Rehm, E. J., Richstone, L., Bulls, Y. M. and Goodman, C. S. (2001). Sidestep encodes a target-derived attractant essential for motor axon guidance in Drosophila. *Cell* **105**, 57-67. doi:10.1016/S0092-8674(01)00296-3

Vactor, D. V., Sink, H., Fambrough, D., Tsoo, R. and Goodman, C. S. (1993). Genes that control neuromuscular specificity in Drosophila. *Cell* **73**, 1137-1153. doi:10.1016/0092-8674(93)90643-5

Winberg, M. L., Mitchell, K. J. and Goodman, C. S. (1998). Genetic analysis of the mechanisms controlling target selection: complementary and combinatorial functions of netrins, semaphorins, and IgCAMs. *Cell* **93**, 581-591. doi:10.1016/S0092-8674(00)81187-3